Photoacoustic assessment of oxygen saturation: effect of red blood cell aggregation

Eno Hysi[a], Ratan K. Saha[b] and Michael C. Kolios[a]
[a]Department of Physics, Ryerson University, Toronto, Canada
[b]Applied Material Science Division, Saha Institute of Nuclear Physics, Kolkata, India;
mkolios@ryerson.ca

ABSTRACT

The simultaneous photoacoustic assessment of oxygen saturation and red blood cell aggregation is presented. Aggregation was induced on porcine red blood cells using Dextran-70 at multiple hematocrit levels. Samples were exposed to 750 nm and 1064 nm for each hematocrit and aggregate size in order to compute the oxygen saturation. As the size of the aggregate increased, the photoacoustic signal amplitude increased monotonically. The same trend was observed for increasing hematocrit at each aggregation level. The oxygen saturation of aggregated samples was 30% higher than non-aggregated samples at each hematocrit level. This suggests that the presence of red blood cell aggregates impairs the release of oxygen to the surrounding environment. Such a result has important implications for detecting red blood cell aggregation non-invasively and making clinical decisions based on the simulatenous assessment of oxygen saturation.

Keywords: Photoacoustics, red blood cell aggregation, oxygen saturation

1. INTRODUCTION

Estimating a patient's need for oxygen is an important assessment of the patient's vital signs as life cannot thrive in the absence of oxygen. Monitoring the oxygen saturation (SO_2) of blood is a routine method for assessing clinical conditions where oxygenation levels fluctuate. The technique is useful in many settings where the patient's oxygenation is unstable (i.e. in intensive care, operating rooms, and emergency or other hospital wards) for determining the effectiveness or need for supplemental oxygen[1]. Typically derived from the hemoglobin concentration, SO_2 is crucially important in mapping brain hemodynamics in various applications such as during responses to sensory simulations[2]. In addition, monitoring of SO_2 has been used to evaluate the treatment of tumors with chemotherapy and radiation therapy[3], monitor the healing of wounds[4] and even study gene expression[5].

Non-invasive monitoring of SO_2 is commonly achieved through the near-infrared spectroscopy (NIRS) method[6]. NIRS relies on 2-wavelength emissions, typically through translucent body parts (i.e. finger tip or earlobes). At the wavelengths typically used (660 nm and 910 nm), the absorption of oxyhemoglobin (OHb) and deoxyhemoglobin (DHb) differs significantly. Therefore, the OHb/DHb ratio can be calculated from the ratio of the absorbance at each respective wavelength. However, a major limitation of NIRS is the small penetration depth due to significant light scattering in tissue. In addition, NIRS is unable to distinguish between venous and arterial blood due to poor spatial resolution[7]. Furthermore, this technique does not provide a complete measure of circulatory sufficiency. It can provide false SO_2 readings based on the blood that arrives at the instant the measurement is taken despite the fact tissue can be hypoxic or hemoglobin insufficient (i.e. anemic)[8].

Photoacoustic (PA) imaging can potentially overcome some of these limitations of NIRS in monitoring SO_2. The primary advantage of PA imaging lies in the fact that the scattering of sound waves detected by passive ultrasonic transducers is 2-3 orders of magnitude smaller than the scattering of light waves thus enabling the probing of deeper structures due to lower attenuation[9]. By using multiple wavelengths of illumination, PA imaging has been able to not

Photons Plus Ultrasound: Imaging and Sensing 2013, edited by Alexander A. Oraevsky, Lihong V. Wang,
Proc. of SPIE Vol. 8581, 85813T · © 2013 SPIE · CCC code: 1605-7422/13/$18 · doi: 10.1117/12.2004960

only measure SO_2 for *in-vivo* samples but also simultaneously form high resolution images using the absorption of the oxygen-carrying cells in circulation, red blood cells (RBCs)[10–12].

Our group has recently shown that the aggregation of RBCs is a phenomenon which affects the PA signals[13,14]. The aggregation of RBCs results in the formation of clusters of RBCs of different sizes which can increase the viscosity of blood and impair the circulation. It is observed in a variety of disorders such as myocardial infarctions, bacterial infections, type 2 diabetes and sickle cell disease[15]. Theoretical simulations showed that as the size of the aggregates increased, the dominant frequency peak of the PA signal power spectrum decreased, approaching the diagnostic frequency range (<30 MHz). This could be attributed to the fact that an aggregate of RBCs behaves as a single entity rather than individual RBCs[13]. Experimentally, we observed that the strength of the PA signal and spectral features of the power spectrum were dependent on the size of the RBC aggregates and that the signal changes correlated well with independent measurements of aggregation[14].

It has been shown that the formation of RBC aggregates contributes to a thickening of the plasma layer around blood aggregates leading to a significant reduction in the diffusion of oxygen in surrounding tissues[16,17]. Since PA techniques are capable of measuring the SO_2 of a blood sample in addition to detecting the presence of aggregation, we propose using PA methods for assessing the effect of RBC aggregation on SO_2. This simultaneous detection could potentially provide a non-invasive method for assessing RBC aggregation and the effect that it has on tissue oxygenation.

2. METHODS

2.1 Sample preparation

The guidelines on handling blood were adapted from the recommendation of the International society for Clinical Hemorheology and the European Society for Clinical Hemorheology and Microcirculation[18]. The source of blood was the femoral vein of Yorkshire pigs (Comparative Research, Toronto, Canada). The blood was drawn into spray-coated EDTA vacutaners (Becton, Dickinson and Company, Franklin Lakes, New Jersey) in order to avoid coagulation. In order to separate the RBCs from the plasma, the blood was centrifuged (1500 g for 6 minutes at room temperature) and then washed twice with phosphate-buffered saline (PBS). The collected, packed RBCs were then suspended in PBS in order to achieve three hematocrit levels (10%, 20% and 40%). Aggregation was induced using Dextran-70 (Sigma-Aldrich, St. Louis, Missouri) dissolved in PBS. Varying degrees of aggregation were achieved by changing the concentration of Dextran in PBS ([Dex-PBS]). In this study, the [Dex-PBS] was 1%, 3% and 8% for each hematocrit level. The blood was kept in full contact with air prior to experimentation and all experiments were completed within 4 hours of blood collection. The presence of aggregation was assessed through light microscopy (Olympus Canada Inc., Markham, Canada). Representative images of non-aggregated and aggregated RBCs are shown in figure 1.

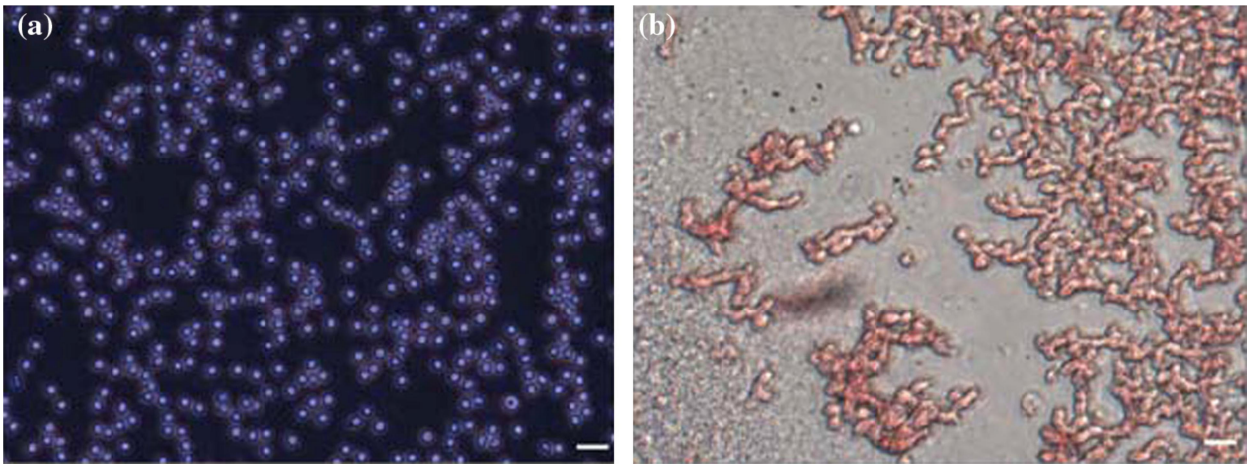

Figure 1: (a) Non-aggregated RBC suspended in PBS and (b) aggregated RBCs suspended in 3% [Dex-PBS]. The scale bar denotes 10 μm.

2.2 PA measurements

The PA measurements were conducted using the Imagio Small Animal PA Imaging Device (Seno Medical Instruments Inc., San Antonio, Texas) shown in figure 2.

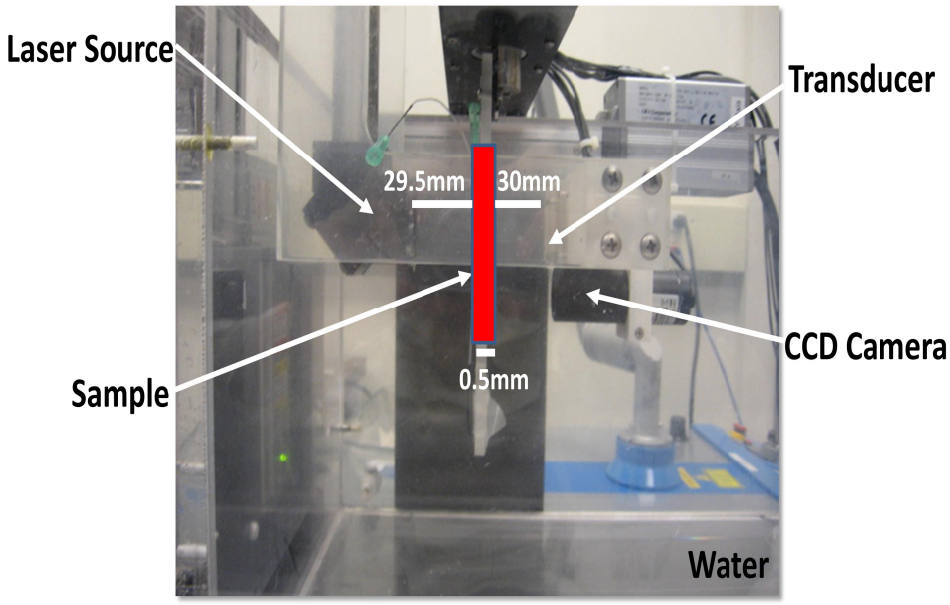

Figure 2: The Imagio Small Animal PA Imaging Device. The blood sample was placed in a cylindrical tube that was placed between the laser (left) and ultrasound transducer (right).

The system consisted of a Q-switched, pulsed Nd:YAG laser delivered through an articulated arm coaxial to a transducer 60 mm apart allowing raster scanning of the sample. The laser beam diameter was 9 mm, the pulse width was 6 ns, the pulse repetition rate was 10 Hz and the maximum fluence was 25 mJ/cm^2/pulse. Each sample was irradiated to 750 nm and 1064 nm lasers. The PA signals were collected through a 4 element annular array transducer with 5 MHz center frequency and 60% -6 dB bandwidth.

The blood samples were loaded into cylindrical tubes (diameter 0.5 mm) at the focus of the transducer (29.5 mm). A vertical raster scan was performed for each sample. During each scan, the laser emitted 4 pulses at each location and the 4 PA signals recorded were averaged to produce 1 PA signal used for analysis. A total of 80 laser pulses were fired for each sample thus corresponding to 20 PA signals at different locations inside each tube (0.5 mm apart over a length of 10 cm).

2.3 Signal analysis and estimation of SO_2

The PA signal amplitude (SA) of each recorded signal was computed as the integration of the Hilbert Transform of the PA signal. The average SA and standard deviation was computed by averaging the SA from all 20 signals recorded for each hematocrit and [Dex-PBS]. The normality of the data was confirmed using a Shapiro-Wilk test (normality criterion $W > 0.05$). An unpaired t-test was used to compare the SA from non-aggregated and aggregated RBCs. Statistical significance was established for p-values of 0.05 or less.

The SO_2 for each exposed sample was computed by taking into account the fact that the SA is directly proportional to the concentration of OHb and DHb[12]. The SO_2 can be computed by exposing each sample at 2 optical wavelengths ($\lambda_1 = 750nm$ and $\lambda_2 = 1064nm$):

$$SO_2 = \frac{[OHb]}{[OHb]+[DHb]} = \frac{SA(\lambda_2)\times\varepsilon(DHb,\lambda_1) - SA(\lambda_1)\times\varepsilon(DHb,\lambda_2)}{SA(\lambda_1)\times\Delta\varepsilon(\lambda_2) - SA(\lambda_2)\times\Delta\varepsilon(\lambda_1)} \quad (1)$$

Here, $\Delta\varepsilon(\lambda) = \varepsilon(OHb,\lambda) - \varepsilon(DHb,\lambda)$ is the difference in extinction coefficient ε for each wavelength of illumination λ.

3. RESULTS AND DISCUSSION

Figure 3 contains the summary of the PA SA of each RBC sample exposed to both illumination wavelengths. The SA is plotted as a function of both hematocrit and aggregation level (determined by the [Dex-PBS]). For both exposure wavelengths, the SA increased monotonically with increasing hematocrit (~1.3x per doubling hematocrit level). This is in accordance to previous reports which suggest that the increase is due to the increase in the concentration of optical absorbers (the RBCs)[13,14,19–21]. The relationship between the PA SA and hematocrit suggests that it might be possible to use PA techniques as a non-invasive means of estimating the hematocrit, an improvement over other non-invasive methods such as ultrasound backscattering where the relationship between the ultrasound backscatter and hematocrit is relatively complex[22].

Increasing aggregation levels resulted in changes in the PA SA as shown in figure 3. For a [Dex-PBS] of 3%, the SA was highest for all hematocrit levels. The 1% and 8% [Dex-PBS] were nearly identical for all hematocrit levels ($p = 0.2$). The SA for the highest aggregation level was ~1.6x higher than the non-aggregated sample (0% [Dex-PBS]) for both wavelengths of illumination ($p = 0.001$). This can be attributed to the fact that the 3% [Dex-PBS] forms the largest aggregate while the 1% and 8% concentrations yield smaller aggregates as previously reported through independent measures of aggregation [23,24]. The SA for the 1064 nm exposure was ~1.3x smaller than the 750 nm exposure for all samples recorded. This could be attributed to the oxygen-depended optical absorption of the RBCs[9].

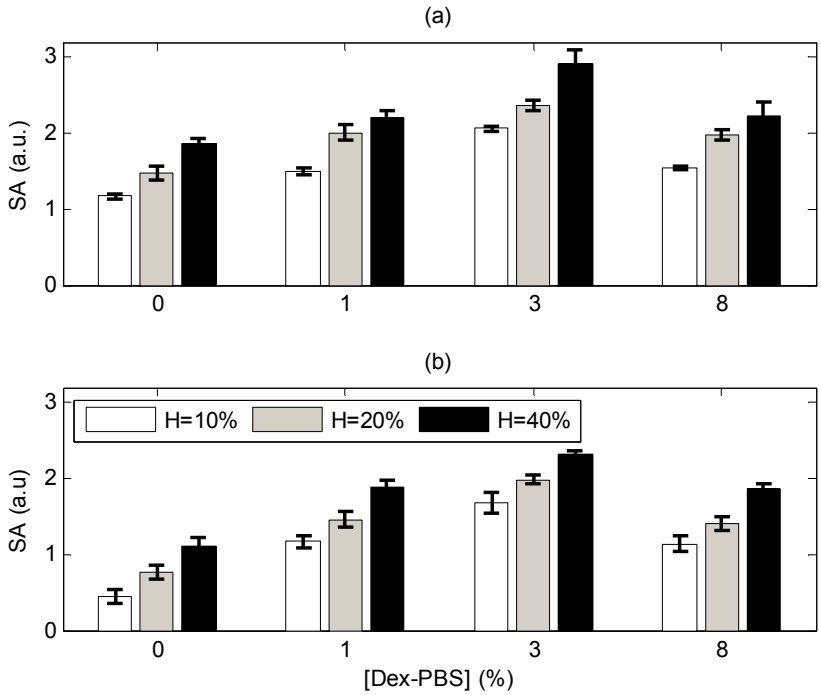

Figure 3: PA SA for (a) 750 nm and (b) 1064 nm exposures of RBC samples at 10%, 20% and 40% hematocrit and 1%, 3% and 8% [Dex-PBS] levels. The 0% [Dex-PBS] corresponds to the non-aggregated sample.

Figure 4 shows the SO_2 computed using equation 1 for the RBC samples examined. A linear increase in the SO_2 with increasing hematocrit was observed with an average increase of ~7% per doubling of the hematocrit level. The largest

SO_2 was recorded for the 3% [Dex-PBS] samples which was ~30% higher than the non-aggregated case ($p = 0.00001$). The 1% and 8% samples were nearly identical and ~20% higher than then non-aggregated samples ($p = 0.00003$). These results suggest that the presence of aggregation increases the SO_2 level. As this oxygen is bound within the aggregate, the ability of the clustered RBCs to release oxygen to the surrounding environment is diminished. This has important implications for adequate oxygen transport to surrounding tissues and further investigations are warranted in order to understand the role of RBC aggregation in vascular pathologies such as atherosclerosis.

Similar increases in SO_2 with aggregation have been reported using a microscope system coupled with a spectrophotometer[17]. The impaired oxygen diffusion due to aggregation is attributed to an increased layer of aggregant/plasma engulfing the RBC aggregates. The fact that PA imaging is capable of measuring changes in oxygenation and RBC aggregation simultaneously suggests that it could potentially be used for making assessments of RBC aggregation in diseased tissues while providing information about the level of oxygen and the capacity of the RBCs to deliver oxygen for the tissues of interest.

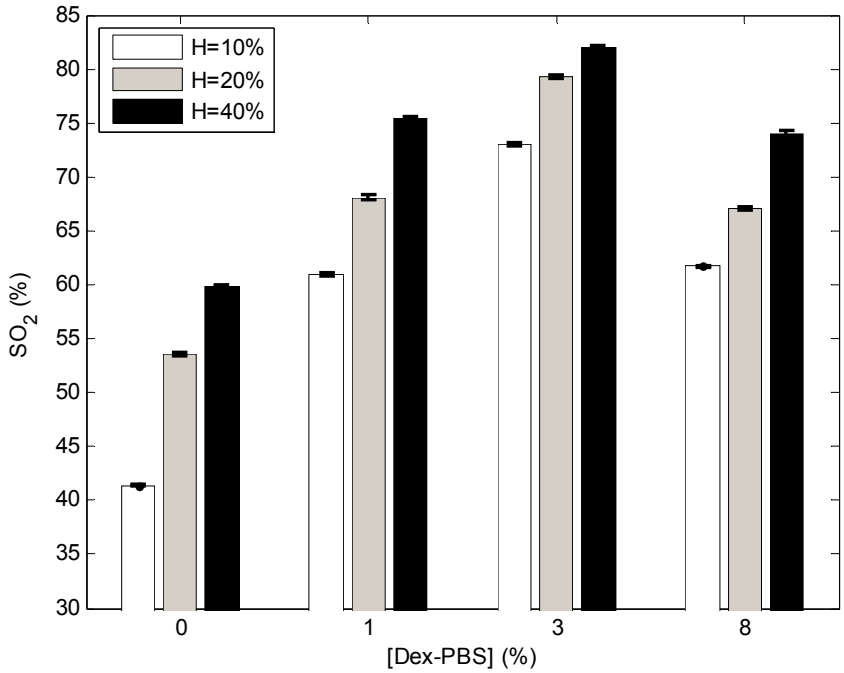

Figure 4: The SO_2 calculated using equation 1 for all blood samples for 3 hematocrit and 3 aggregation levels. The 0% [Dex-PBS] corresponds to the non-aggregated sample.

4. CONCLUSIONS

This paper presents the potential for using PA techniques for assessing oxygenation of blood samples in the presence of RBC aggregates. The results of this study suggest that in the presence of RBC aggregation, the release of oxygen to the surrounding environment is impaired. It might be possible to use PA imaging for assessing the presence of RBC aggregation in circulatory disorders while measuring the oxygenation of the same area and thereby monitoring the need for oxygen to the surrounding tissues.

ACKNOWLEDGEMENTS

This work was made possible due to the financial support of the following granting agencies awarded to M. C. Kolios: Natural Sciences and Engineering Research Council of Canada, Canadian Institutes of Health Research, Canadian Foundation for Innovation, Canada Research Chairs Program and the Terry Fox Foundation. E. Hysi was supported

through the Alexander Graham Bell Graduate Scholarship. A. Worthington is gratefully acknowledged for the technical support provided along with J. Barry for providing the porcine blood. The authors are also very thankful to M. Rui and E. Berndl for their assistance with the blood specimens.

REFERENCES

[1] C.D Hanning and J. M. Alexander-Williams, "Pulse oximetry: a practical review," Brit. Med. J. 311, 367-370 (1995).

[2] H. F. Zhang et al., "Imaging of hemoglobin saturation variation in single vessels in vivo using photoacoustic microscopy," Appl. Opt. 90(5), 053901 (2007).

[3] M. Henke et al., "Blood hemoglobin level may affect radiosensitivitypreliminary results on acutely reacting normal tissues," Int. J. Radiat. Oncol. Biol. Phys. 48(2), 339–345 (2000).

[4] B. Venkatesh et al., "Monitoring tissue oxygenation during resuscitation of major burns," J. Trauma 50(3), 485–494 (2001).

[5] S. S. Foo et al., "Functional imaging of intratumoral hypoxia," Mol. Imaging. Biol. 6(5), 291–305 (2004).

[6] M. E. George et al., "Noninvasive tissue oxygen saturation measurements identify supply dependency," J. Surg. Res. 160, 40-46 (2010).

[7] S. Hu and L. V. Wang, "Photoacoustic imaging and characterization of microvasculature," J. Biomed. Opt. 15(1), 011101 (2010).

[8] K. Maslov et al., "Effects of wavelength-dependent fluence attenuation of the noninvasive photoacoustic imaging of hemoglobin oxygen saturation of subcutaneous microvasculature in vivo," Inverse Probl. 23, S113-S122 (2007).

[9] L. V. Wang, "Prospects of photoacoustic tomography," Med. Phys. 35(12), 5758–2767 (2008).

[10] C. Li and L. V. Wang, "Photoacoustic tomography and sensing in biomedicine," Phys. Med. Biol. 54(19), R59–R97 (2009).

[11] Y. Wang et al., "In vivo intergrated photoacoustic and confocal microscopy of hemoglobin oxygen saturation and oxygen partial pressure," Opt. Let. 36(7), 1029-1031 (2011).

[12] X.Wang et al., "Noninvasive imaging of hemoglobin concentration and oxygenation in rat brain using high-resolution photoacoustic tomography," J. Biomed. Opt. 11(2), 024015 (2006).

[13] R. K. Saha and M. C. Kolios, "A simulation study on photoacoustic signals from red blood cells," J. Acoust. Soc. Am. 129(5), 2935-2943, (2011).

[14] E. Hysi, R. K. Saha, and M. C. Kolios, "On the use of photoacoustics to detect red blood cell aggregation," Biomed. Opt. Express 3(9), 2326– 2338 (2012).

[15] O. K. Baskurt, B. Neu, and H. J. Meiselman, Red Blood Cell Aggregation, pp. 1–304, CRC Press, Boca Raton, FL (2011).

[16] N. Tateishi et al., "Reduced oxygen release from erythrocytes by the acceleration-induced flow shift, observed in an oxygen-permable narrow tube," J. Biomech. 35(9), 1241–1251 (2002).

[17] N. Tateishi, N. Maeda, and T. Shiga, "A method for measuring the rate of oxygen release from single microvessels," Circ. Res. 70(4), 812–819 (1992).

[18] O. K. Baskurt et al., “New guidelines for hemorheological laboratory techniques,” Clin. Hemorheol. Micro. 42(2), 75–97 (2009).

[19] R. K. Saha and M. C. Kolios, “Effects of erythrocyte oxygenation on optoacoustic signals,” J. Biomed. Opt. 16(11), 115003 (2011).

[20] E. Hysi et al., “Photoacoustic ultrasound spectroscopy for assessing red blood cell aggregation and oxygenation,” J. Biomed. Opt. 17(12), 125006 (2012).

[21] A. B. Karpiouk et al., “Combined ultrasound and photoacoustic imaging to detect and stage deep vein thrombosis: phantom and ex vivo studies,” J. Biomed. Opt. 13(5), 055406 (2008).

[22] R. S. C. Cobbold, Foundations of Biomedical Ultrasound, pp. 100–123, Oxford University Press, New York, NY (2007).

[23] O. K. Baskurt, R. A. Farley, and H. J. Meisleman, “Erythrocyte aggregation tendency and cellular properties in horse, human, and rat: a comparative study,” Am. J. Physiol. Heart Circ. Physiol. 273, H2604–H2612 (1997).

[24] O. K. Baskurt et al., Handbook of Hemorheology and Hemodynamics, pp. 1–455, IOS Press, Amsterdam (2007).